Supporting information for

Theoretical Investigation of a Vital Step in the Gas-phase Formation of Interstellar Ammonia: $NH_2^+ + H_2 \rightarrow NH_3^+ + H$

Salvi Mohandas[1], Raghunath O. Ramabhadran[2], and S. Sunil Kumar[1]**

[1]Department of Physics and Center for Atomic, Molecular, and Optical Sciences & Technologies, Indian Institute of Science Education and Research (IISER) Tirupati, Tirupati 517507, Andhra Pradesh, India

[2]Department of Chemistry and Center for Atomic, Molecular, and Optical Sciences & Technologies, Indian Institute of Science Education and Research (IISER) Tirupati, Tirupati 517507, Andhra Pradesh, India

List of figures and tables

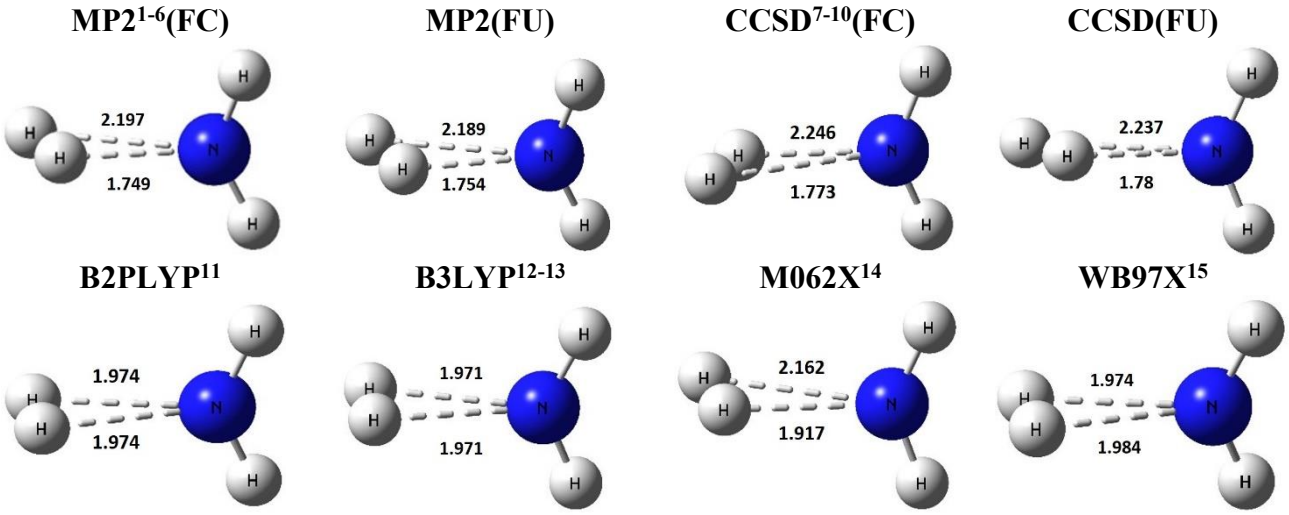

Figure S1. Transition state geometries determined in different methods/levels of theory performed using aug-cc-pVTZ[16] basis set. The bond distances between the nitrogen atom and the two hydrogen atoms in the H_2 molecule are shown.

Table S1. Transition state geometries in their z-matrix format determined in different methods/levels of theory performed using aug-cc-pVTZ basis set. The labels are according to the configuration as shown below for a transition state. In the representation 'R' corresponds to bond distance, 'A' angle and 'D' for the dihedral angle between the following numbered atoms in the molecule.

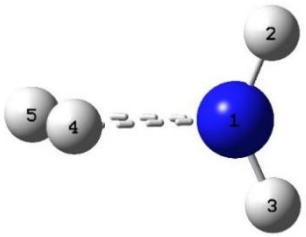

MP2			MP2(FU)			CCSD			CCSD(FU)		
R12	=	1.0246	R12	=	1.02109	R12	=	1.0270	R12	=	1.0232
R13	=	1.0246	R13	=	1.02109	R13	=	1.0270	R13	=	1.0232
A213	=	134.4520	A213	=	134.5973	A213	=	135.86652	A213	=	136.0150
R14	=	1.7493	R14	=	1.7544	R14	=	1.7734	R14	=	1.78
A214	=	112.578	A214	=	112.5012	A214	=	111.9077	A214	=	111.8269
D3214	=	172.1074	D3214	=	171.97189	D3214	=	172.7684	D3214	=	172.6079
R45	=	0.7726	R45	=	0.7720	R45	=	0.7766	R45	=	0.7761
A145	=	15.6883	A145	=	114.377	A145	=	118.0589	A145	=	116.5280
D2145	=	93.047	D2145	=	93.0896	D2145	=	92.7111	D2145	=	92.7616
B2PLYP			**B3LYP**			**M062X**			**ω −B97XD**		
R12	=	1.0264	R12	=	1.02886	R12	=	1.0282	R12	=	1.0262
R13	=	1.0264	R13	=	1.02886	R13	=	1.0284	R13	=	1.0262
A213	=	133.47	A213	=	131.6673	A213	=	136.7651	A213	=	133.0832
R14	=	1.9741	R14	=	1.9706	R14	=	1.9167	R14	=	1.9671
A214	=	112.7862	A314	=	113.6530	A314	=	110.4209	A314	=	109.8185
D3214	=	167.7017	D2314	=	167.45146	D2314	=	70.2769	D2314	=	166.9207
R45	=	0.7758	R45	=	0.7845	R45	=	0.7692	R45	=	0.7801
A145	=	78.7120	A145	=	78.5392	A145	=	97.9696	A145	=	79.4513
D2145	=	94.8261	D2145	=	95.1029	D2145	=	86.2075	D2145	=	79.0124

Table S2. The geometries of species in their z-matrix format determined in MP2 method/level of theory performed using aug-cc-pVTZ basis set. The corresponding spin states are given in bracket.

H_2(0)			NH_2^+(3)		
R12	=	0.73743800	R12	=	1.02840899
			R13	=	1.02840899
			A213	=	150.38348614
RX(3)			**TS(3)**		
R12	=	1.02664521	R12	=	1.02458448
R13	=	1.02664521	R13	=	1.02458448
A213	=	146.39325042	A213	=	134.45207276
R14	=	2.38897159	R14	=	1.74936311
A214	=	106.59117269	A214	=	112.57997132
D3214	=	170.62104068	D3214	=	172.10740181
R45	=	0.74621400	R45	=	0.77245688
A145	=	81.01482394	A145	=	115.68828816
D2145	=	92.70025329	D2145	=	93.04698099
PX(3)			NH_3^+(2)		
R12	=	1.01944093	R12	=	1.01971013
R13	=	1.01944014	R13	=	1.01970929
A213	=	119.68457493	A213	=	120.00003747
R14	=	1.02557000	R14	=	1.01971013
A214	=	120.15769466	A214	=	119.99996629
D3214	=	179.99993538	D3214	=	180.00000000
R15	=	2.97467000			
A415	=	0.00017667			
D2415	=	161.56508364			

Table S3. The geometry of the reactant, NH_2^+, the product , NH_3^+ and the transition state, TS in z-matrix format determined in MP2 method/level of theory using aug-cc-pVTZ basis set. The corresponding spin states are given in bracket.

NH_2^+ (1)			NH_3^+ (4)		
R12	=	1.0427	R12	=	1.0449
R13	=	1.0427	R13	=	1.0248
A213	=	107.5252	A213	=	157.0139
			R14	=	2.6656
			A214	=	2.7960
			D3214	=	179.88585688
TS **(1)**					
R12	=	1.0339			
R13	=	1.0339			
A213	=	105.9851			
R14	=	1.1016			
A314	=	99.4489			
D2314	=	102.7564			
R45	=	0.8673			
A145	=	179.9993			
D2145	=	37.4486			

Cartesian coordinates of the transition state (MP2[1-6]/aug-cc-pVTZ[7])

N	0.28221700	0.00000000	-0.00083800
H	0.67789000	0.94470700	-0.02813100
H	0.67789000	-0.94470700	-0.02813100
H	-1.43365100	0.00000000	0.33985000
H	-1.89764800	0.00000000	-0.27772300

Cartesian coordinates of the reactant NH_2^+ (MP2/aug-cc-pVTZ)

N	0.00000000	0.00000000	0.05841000
H	0.00000000	0.99425200	-0.20443600
H	0.00000000	-0.99425200	-0.20443600

Cartesian coordinates of the reactant H_2 (MP2/aug-cc-pVTZ)

H	0.00000000	0.00000000	0.00000000
H	0.00000000	0.00000000	0.73744000

Cartesian coordinates for the product NH_3^+ (MP2/aug-cc-pVTZ)

N	0.00000000	0.00000000	0.00000000
H	-0.88118200	0.51315400	0.00000000
H	0.88499500	0.50654800	0.00000000
H	-0.00381400	-1.01970300	0.00000000

Cartesian coordinates for the reactant complex (MP2/aug-cc-pVTZ)

N	-0.37506600	0.00000000	0.00000000
H	-0.67185700	0.98281000	0.00000000
H	-0.67185700	-0.98281000	0.00000000
H	1.98459000	0.00000000	-0.37310700
H	1.98459000	0.00000000	0.37310700

Cartesian coordinates for the product complex (MP2/aug-cc-pVTZ)

N	0.27054000	0.00000000	0.00000000
H	0.78269100	0.88145400	0.00000000
H	0.78268600	-0.88145600	0.00000000
H	-0.75503000	0.00000300	0.00000100
H	-2.70413000	0.00000000	0.00000000

Table S4. The electronic energy, zero-point energy of the H_2 molecule (singlet spin state) in different levels of theory in computed aug-cc-pVTZ basis-set using harmonic analysis.

Method	Zero-point energy (kJ/mol)	Zero-point energy corrected electronic energy (kJ/mol)	Absolute electronic energy (kJ/mol)
MP2	27.02	-3031.746	-3058.768
MP2(FU)	27.02	-3031.746	-3058.768
CCSD	26.32	-3052.430	-3078.754
CCSD(FU)	26.32	-3052.430	-3078.754

Table S5. The electronic energy, zero-point energy of the NH_2^+ (triplet spin state) molecule in different levels of theory in computed aug-cc-pVTZ basis-set using harmonic analysis.

Method	Zero-point energy (kJ/mol)	Zero-point energy corrected electronic energy (kJ/mol)	Absolute electronic energy (kJ/mol)
MP2	45.99	-145323.4	-145369.4
MP2(FU)	46.29	-145363.3	-145409.6
CCSD	45.12	-145374.4	-145419.5
CCSD(FU)	45.47	-145414.8	-145460.3

Table S6. The electronic energy, zero-point energy of the transition state (triplet spin state) in different levels of theory in computed aug-cc-pVTZ basis-set using harmonic analysis.

Method	Zero-point energy (kJ/mol)	Zero-point energy corrected electronic energy (kJ/mol)	Absolute electronic energy (kJ/mol)
MP2	81.710	-148352.1	-148433.8
MP2(FU)	82.30	-148392.3	-148474.6
CCSD	80.38	-148425.3	-148505.7
CCSD(FU)	81.00	-148466.2	-148547.2

Table S7. The electronic energy, zero-point energy of the NH_3^+ (doublet spin state) product molecule in different levels of theory in computed aug-cc-pVTZ basis-set using harmonic analysis.

Method	Zero-point energy (kJ/mol)	Zero-point energy corrected electronic energy (kJ/mol)	Absolute electronic energy (kJ/mol)
MP2	87.11	-147161.6	-147248.7
MP2(FU)	87.75	-147205.2	-147292.9
CCSD	86.61	-147211.3	-147297.9
CCSD(FU)	87.34	-147255.6	-147343.0

Table S8. The electronic energy including the zero-point energy (in kJ/mol) of all the species involved in the reaction of interest computed in MP2(FU) level of theory in different basis sets, aug-cc- pVDZ[17], aug-cc-pVTZ and aug-cc- pVQZ[18].

Method	APVDZ	APVTZ	APVQZ
H_2	-3008.954	-3031.743	-3036.26
NH_2^+	-145221.0	-145363.3	-145432.2
RX	-148233.2	-148398.1	-148471.5
TS	-148228.3	-148392.3	-148466.4
PX	-148353.7	-148521.4	-148596.1
NH_3^+	-147039.6	-147205.2	-147279.8
H	-1311.0	-1312.3	-1312.6

(Note: RX – reactant complex, TS- transition state, PX- product complex)

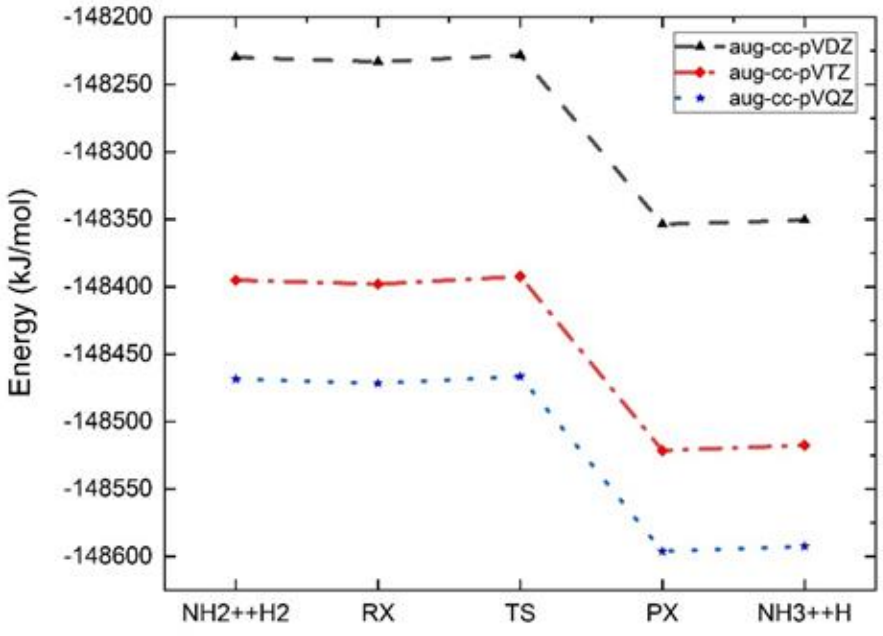

Figure S2. The electronic energy diagram including the zero-point energy of all the species involved in the reaction of interest computed in MP2(FU) level of theory in different basis sets, aug-cc-pVDZ, aug-cc-pVTZ and aug-cc-pVQZ.

Table S9. The electronic energy, zero-point energy of the NH_2^+ (singlet spin state), transition state (singlet) and product NH_3^+ (quadruplet) molecule computed MP2(FU) method with aug-cc-pVTZ basis-set using harmonic analysis.

Method	Zero-point energy (kJ/mol)	Zero-point energy corrected electronic energy (kJ/mol)	Absolute electronic energy (kJ/mol)
$\boldsymbol{NH_2^+}$	48.17791838	-145212.0503	-145260.2282
TS	93.88261609	-148420.4582	-148514.3408
$\boldsymbol{NH_3^+}$	51.28913545	-146685.5752	-146736.8643

Table S10. Zero-point-corrected energies of species involved in the reaction in different spin state. The charge and spin multiplicity are given in brackets.

Optimized in MP2/aug-cc-pVTZ	Energy (Hartree)	Energy (Hartree)
$\boldsymbol{H_2}$	**-1.15473 (0 1)**	**-0.99965 (0 3)**
$\boldsymbol{NH_2^+}$	**-55.35077(1 3)**	**-55.29379 (1 1)**
$\boldsymbol{H_2 + NH_2^+}$	**-56.5055**	**-56.29344**
$\boldsymbol{TS}$	**-56.50433 (1 3)**	**-56.51794 (1 1)**
$\boldsymbol{NH_3^+ + H}$	**-56.55068**	**-56.35088**
$\boldsymbol{NH_3^+}$	**-56.05089 (1 2)**	**-55.85109 (1 4)**
$\boldsymbol{H}$	**-0.49979 (0 2)**	**-0.49979 (0 2)**

Table S11. The magnitude of different frequency modes of vibration of the transition state in different levels of theory with aug-cc-pVTZ basis-set using harmonic analysis.

Method	Frequency ($\boldsymbol{cm^{-1}}$)								
	1	**2**	**3**	**4**	**5**	**6**	**7**	**8**	**9**
MP2	684.69i	169.06	417.78	514	599.57	1158.63	3365.49	3596.3	3840.01
MP2(FU)	668.22i	186.78	414.16	518.84	604.58	1166.14	3400.85	3614.02	3853.3
CCSD	601.97i	166.9	417.92	499.09	582.76	1115.4	3331.91	3557.44	3766.7
CCSD(FU)	584i	182.05	414.25	502.93	587.3	1123.42	3371.15	3577.45	3783.34
B2-PLYP	353.0i	204.0	456.70	513.78	634.94	1133.59	3323.97	3551.17	3932.35
B3-LYP	480.3i	206.91	466.93	589.14	660.45	114.57	3290.53	3512.06	3844.76
M06-2X	706.82i	386.74	440.5	526.28	751.13	1087.35	3333.92	3568.33	3958.34
ω-B97XD	427.35i	287.35	468.67	557.17	625.47	1143.88	3348.36	3576.08	3915.70

Table S12. The magnitude of different frequency mode of vibration of the H_2 molecule in different levels of theory in computed aug-cc-pVTZ basis-set using harmonic analysis

Method	Frequency (cm^{-1})
MP2	4517.65
MP2(FU)	4517.65
CCSD	4401.15
CCSD (FU)	4401.15

Table S13. The magnitude of different frequency mode of vibration of the NH_2^+ reactant molecule in different levels of theory in computed aug-cc-pVTZ basis-set using harmonic analysis

Method	Frequency (cm^{-1})		
	1	**2**	**3**
MP2	816.38	3306.45	3567.11
MP2(FU)	814.62	3343.67	3581.39
CCSD	750.5	3269.91	3523.62
CCSD (FU)	750.82	3311.41	3539.09

Table S14. The magnitude of different frequency mode of vibration of the $NH_2^+ \cdot H_2$ reactant complex in different levels of theory in computed aug-cc-pVTZ basis-set using harmonic analysis.

Method	Frequency (cm^{-1})								
	1	**2**	**3**	**4**	**5**	**6**	**7**	**8**	**9**
MP2	154.75	189.3	219.41	283.77	432.74	896.57	3328.36	3587.46	4363.63
MP2(FU)	155.62	199.29	218.23	290.09	429.09	901.78	3364.18	3602.69	4359.12
CCSD	159.55	222.42	222.80	326.96	419.82	872.94	3297.37	3547.08	4227.01
CCSD(FU)	160.53	220.84	235.84	337.47	414.42	885.04	3337.62	3564.76	4216.29

Table S15. The magnitude of different frequency mode of vibration of the NH_3^+.H product complex in different levels of theory in computed aug-cc-pVTZ basis-set using harmonic analysis.

Method	Frequency (cm^{-1})								
	1	**2**	**3**	**4**	**5**	**6**	**7**	**8**	**9**
MP2	167.49	241.5	312.55	855.46	1555.69	1562.15	3352.58	3537.76	3602.47
MP2(FU)	183.49	270.95	315.7	872.28	1568.39	1578.25	3385.26	3550.69	3614.59
CCSD	171.21	247.45	319.66	870.38	1552.54	1559.16	3323.64	3503.2	3568.6
CCSD(FU)	188.28	279.64	322.18	887.48	1566.9	1577.24	3360.1	3518.41	3582.71

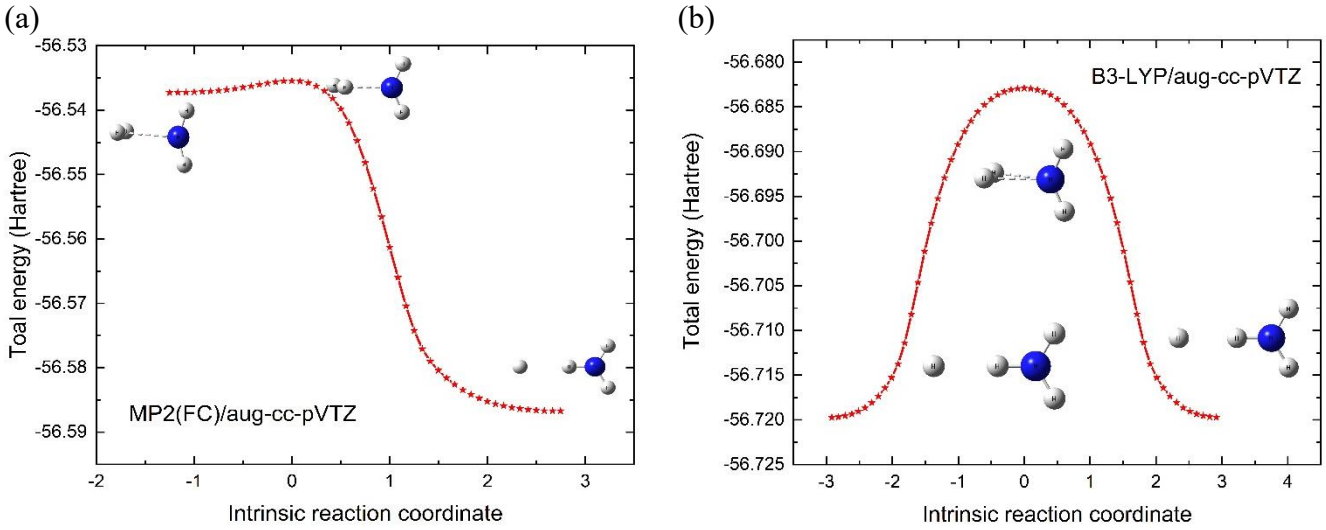

Figure S3. The minimum energy path (IRC) connecting the reactant complex, the transition state, and the product complex computed using MP2(FC) and B3-LYP levels of theory in aug-cc-pVTZ basis set. Nature of the species on either side of the transition state indicates that the TS does not correspond to the reaction of concern.

Table S16. The magnitude of different frequency mode of vibration of the NH_3^+ product in different levels of theory in computed aug-cc-pVTZ basis-set using harmonic analysis.

Method	Frequency (cm^{-1})					
	1	**2**	**3**	**4**	**5**	**6**
MP2	837.73	1559	1559	3408.2	3598.9	3598.9
MP2(FU)	855.05	1574.94	1574.94	3439.76	3613.24	3613.24
CCSD	852.3	1555.88	1555.89	3385.36	3565.4	3565.41
CCSD (FU)	869.87	1573.8	1573.8	3420.57	3582.06	3582.06

Table S17. The normal modes of vibration determined in MP2 method/level of theory using aug-cc-pVTZ basis set for reactant, transition state and product at the specified spin state.

Species	Frequency (cm^{-1})								
	1	**2**	**3**	**4**	**5**	**6**	**7**	**8**	**9**
NH_2^+ (singlet)	1445.2	3269.0	3340.	-	-	-	-	-	-
TS (singlet)	1452.9i	1083.9i	1147.2	1253.1	1487.8	1649.4	3326.7	3408.4	3423.4
NH_3^+ (quadruplet)	334.4	465.7	510.4	723.0	3042.3	3499.3	-	-	-

Table S18. The activation energy (E_a) in kJ/mol in terms absolute electronic energy and electronic energy including the zero-point energy computed using different levels of theory in aug-cc-pVTZ basis set.

Method	Without ZPE	With ZPE
MP2	-5.6	3.1
MP2 (FU)	-6.3	2.7
CCSD	-7.4	1.5
CCSD(FU)	-8.1	1.1

Table S19. The activation energy (E_a) in kJ/mol in terms absolute electronic energy and electronic energy including the zero-point energy computed MP2(FU) levels of theory in different basis set.

Basis set	Without ZPE	With ZPE
aug-cc-pVDZ	-7.3	1.7
aug-cc-pVTZ	-6.3	2.7
aug-cc-pVQZ	-7.0	2.0

Table S20. The activation energy (E_a) in kJ/mol in terms absolute electronic energy and electronic energy including the zero-point energy computed MP2(FC) levels of theory in different basis set.

Basis set	Without ZPE	With ZPE
aug-cc-pVDZ	-7.0	2.0
aug-cc-pVTZ	-5.6	3.1
aug-cc-pVQZ	-6.5	2.4

Table S21. The activation energy (E_a) in kJ/mol in terms absolute electronic energy and electronic energy including the zero-point energy computed at CCSD(FU) levels of theory using different basis sets.

Basis set	Without ZPE	With ZPE
aug-cc-pVDZ	-8.7	0.3
aug-cc-pVTZ	-8.1	1.1
aug-cc-pVQZ	-8.8	0.5

Table S22. The activation energy (E_a) in kJ/mol in terms absolute electronic energy and electronic energy including the zero-point energy computed at CCSD levels of theory using different basis sets.

Basis set	Without ZPE	With ZPE
aug-cc-pVDZ	0.0	0.5
aug-cc-pVTZ	0.0	1.5

Table S23. Activation energies (E_a) in kJ/mol computed in CCSD(T)[19,20] methods with and without core electron contributions in aug-cc-pV5Z[21] basis set are listed in the table. The electronic energy values are from single point energy calculations in aug-cc-pV5Z basis set. The geometry and the zero-point energy are chosen from a MP2 or CCSD method as mentioned in the table.

Method	Without ZPE	With ZPE
CCSD(T)[1]/aug-cc-pV5Z //MP2/aug-cc-pVTZ	-12.2	-3.5
CCSD(T)(FU)/aug-cc-pV5Z //MP2(FU)/aug-cc-pVTZ	-12.8	-3.8
CCSD(T)/aug-cc-pV5Z //CCSD/aug-cc-pVTZ	-12.0	-3.0
CCSD(T)(FU)/aug-cc-pV5Z //CCSD(FU)/aug-cc-pVTZ	-12.5	-3.3

Table S24. The activation energy (E_a) in kJ/mol from CBS electronic energy and CBS electronic energy including the zero-point energy from the respective optimized geometry. CBS exponential extrapolation is carried out for electronic energies from SP calculation at CCSD(T) level of theory with aug-cc-pVTZ, QZ, 5Z and 6Z basis sets for the geometries specified in the table.

Basis set	Without ZPE	With ZPE
CCSD(T)/CBS// MP2/aug-cc-pVTZ	-16.6	-7.9
CCSD(T)/CBS//CCSD/aug-cc-pVTZ	-12.0	-3.1
CCSD(T)(FU)/CBS// MP2(FU)/aug-cc-pVTZ	-3.0	5.9
CCSD(T)(FU)/CBS// CCSD(FU)/aug-cc-pVTZ	-11.8	-2.5

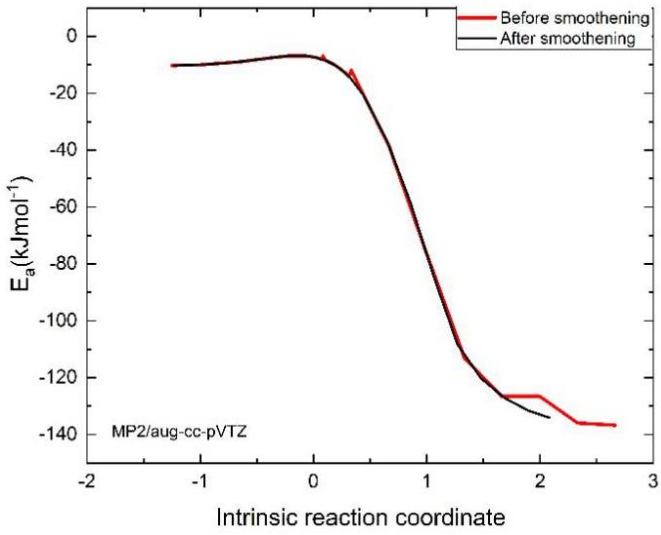

Fig. S4. The activation energy variation along the IRC is plotted before and after smoothening computed at MP2(FU)/aug-cc-pVTZ level of theory.

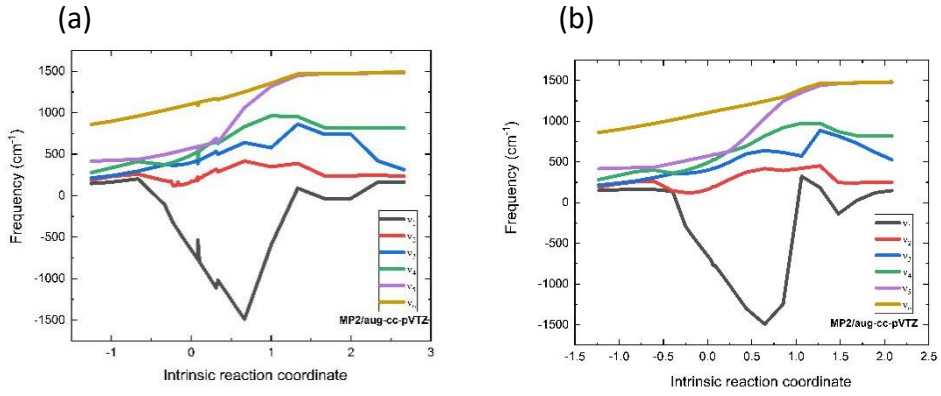

Fig. S5. The frequency variation along IRC (a) before and (b) after smoothening. The different modes of frequencies are computed at MP2(FU)/aug-cc-pVTZ level of theory.

Table S25. Rate coefficients at different temperature with transition-state theory with and without Wigner-tunneling correction and variational transition-state theory with Wigner-tunneling correction at MP2(FU)/ aug-cc-pVTZ level.

Temperature (K)	Rate (TST) ($cm^3molec^{-1}s^{-1}$)	Rate (TST with tunneling)($cm^3molec^{-1}s^{-1}$)	Rate (VTST with tunneling)($cm^3molec^{-1}s^{-1}$)
10	1.98E-12	6.92E-10	6.92E-10
20	4.66E-11	4.12E-09	4.08E-10
30	1.03E-10	4.10E-09	8.91E-10
40	1.35E-10	3.08E-09	9.90E-10
50	1.48E-10	2.21E-09	8.98E-10
60	1.50E-10	1.60E-09	7.62E-10
70	1.47E-10	1.19E-09	6.34E-10

80	1.42E-10	9.17E-10	5.29E-10
90	1.37E-10	7.25E-10	4.46E-10
100	1.31E-10	5.88E-10	3.81E-10
110	1.26E-10	4.88E-10	3.31E-10
120	1.21E-10	4.14E-10	2.91E-10
130	1.17E-10	3.58E-10	2.59E-10
140	1.13E-10	3.14E-10	2.34E-10
150	1.10E-10	2.80E-10	2.14E-10
160	1.07E-10	2.53E-10	1.97E-10
170	1.05E-10	2.31E-10	1.84E-10
180	1.03E-10	2.13E-10	1.73E-10
190	1.01E-10	1.98E-10	1.64E-10
200	9.94E-11	1.86E-10	1.56E-10
210	9.83E-11	1.76E-10	1.50E-10
220	9.74E-11	1.68E-10	1.44E-10
230	9.67E-11	1.60E-10	1.40E-10
240	9.62E-11	1.54E-10	1.36E-10
250	9.58E-11	1.49E-10	1.33E-10
260	9.57E-11	1.45E-10	1.31E-10
270	9.56E-11	1.41E-10	1.29E-10
280	9.57E-11	1.38E-10	1.27E-10
290	9.59E-11	1.36E-10	1.26E-10
300	9.63E-11	1.34E-10	1.25E-10

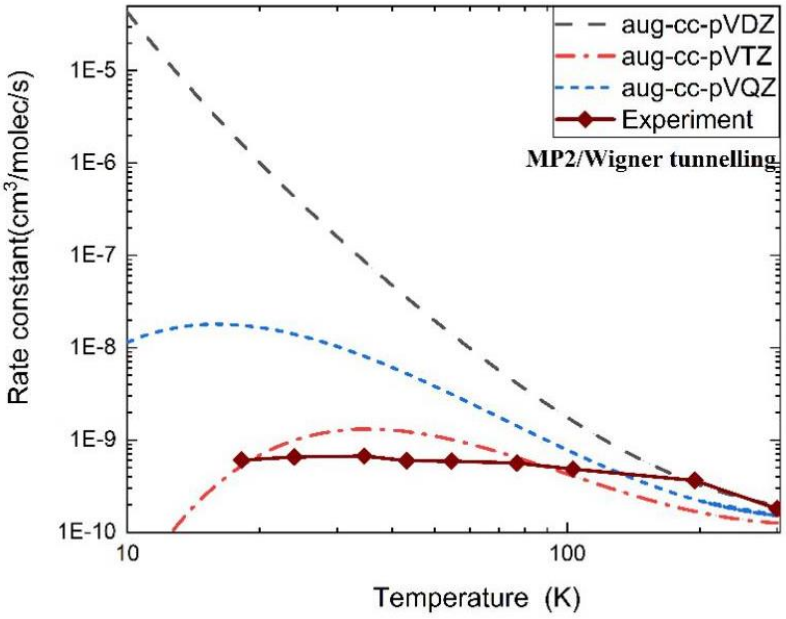

Fig. S6. The rate constant variation with temperature at MP2 level of theory with three basis sets are plotted along with the experimental one. The rate constant converges at room temperature irrespective of the basis-set used, but considerably different at lower temperature. The curves follow barrier height order as given in the table S20.

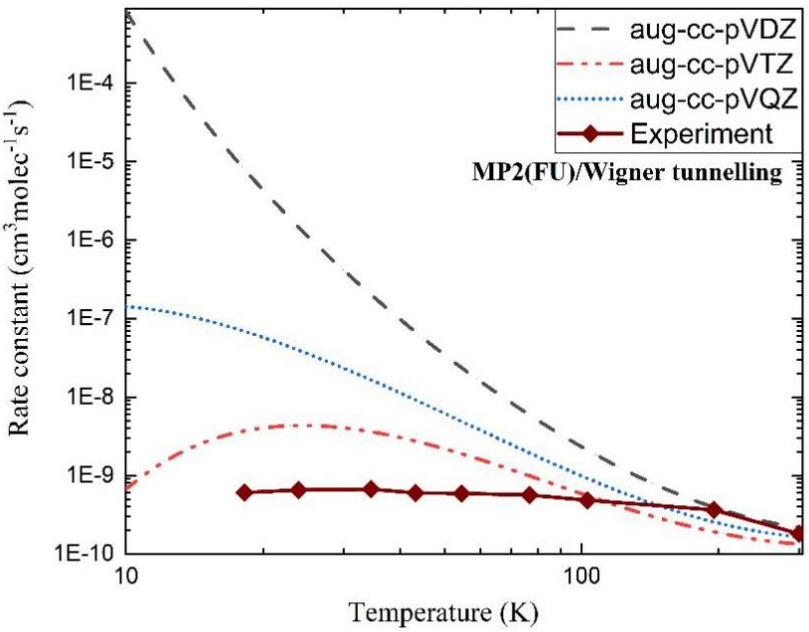

Fig. S7. The rate constant variation with temperature at MP2(FU) level of theory in three basis sets are plotted along with the experimental one. The rate constant converges at room temperature irrespective of the basis-set used, but considerably different at lower temperature. Out of the three, aug-cc-pVTZ gives the highest barrier height, then aug-cc-pVQZ and lowest is for aug-cc-pVDZ.

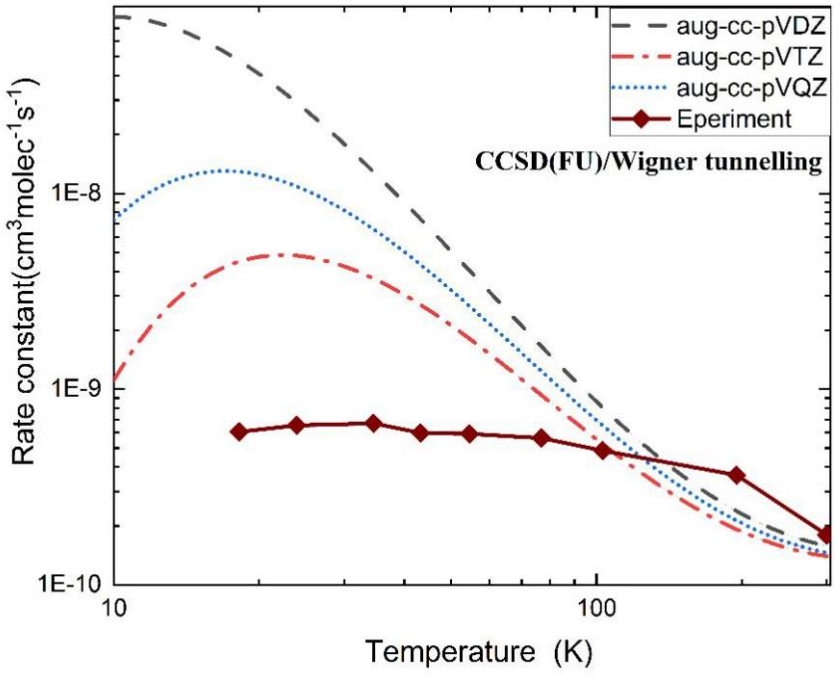

Fig. S8. The rate constant variation with temperature at CCSD(FU) level of theory in three basis sets are plotted along with the experimental one. The rate constant converges at room temperature irrespective of the basis-set used, but

considerably different at lower temperature. Here again, the behaviour follows as trend as for MP2 and MP2(FU) calculation.

Table S26. The value of vibrational scaling factors used for different levels of theory and corresponding basis set[23].

Method	MP2	MP2(FU)	CCSD	CCSD(FU)
aug-cc-pVDZ	0.959	0.969	0.963	--
aug-cc-pVTZ	0.953	0.951	0.956	0.951
aug-cc-pVQZ	0.950	0.956	--	--

References

1. Møller, C.; Plesset, M. S. Note on an approximation treatment for many-electron systems, *Phys. Rev.* **1934**, *46*, 0618-22.
2. Saebø, S.; Almlöf, S. Avoiding the integral storage bottleneck in LCAO calculations of electron correlation, *Chem. Phys. Lett.* **1989,** *154,* 83-89.
3. Head-Gordon, M.; Head-Gordon, T. Analytic MP2 frequencies without Fifth order storage: theory and application to bifurcated hydrogen bonds in the water hexamer, *Chem. Phys. Lett.* 1**994**, *220*,122-28.
4. Head-Gordon, M.; Pople, J. A.; Frisch, M. J. MP2 energy evaluation by direct methods, *Chem. Phys. Lett.*, **1988**, *153*, 503-06.
5. Frisch, M. J.; Head-Gordon, M.; Pople, J. A. Semi-direct algorithms for the MP2 energy and gradient, *Chem. Phys. Lett.* **1990**, *166*, 281-89.
6. Frisch, M. J.; Head-Gordon, M.; Pople, J. A. Direct MP2 gradient method, *Chem. Phys. Lett.* **1990**, *166*, 275-80.
7. Scuseria, G. E.; Schaefer III, H. F. Is coupled cluster singles and doubles (CCSD) more computationally intensive than quadratic configuration-interaction (QCISD)? *J. Chem. Phys.* **1989,** 90, 3700-03.
8. Scuseria, G. E.; Janssen, C. L.; Schaefer III, H. F. An efficient reformulation of the closed-shell coupled cluster single and double excitation (CCSD) equations, *J. Chem. Phys.* **1988**, 89, 7382-87.
9. Purvis III, G. D. ; Bartlett, R. J. A full coupled-cluster singles and doubles model – the inclusion of disconnected triples, *J. Chem. Phys.* **1982**, *76*, 1910-18.
10. Cížek, J.; In *Advances in Chemical Physics;* Hariharan, P. C., Ed.; Wiley Interscience, New York, **1969** , Vol. 14, 35.
11. Gimme, S. Semiempirical Hybrid Density Functional with Perturbative Second-Order Correlation. *J.Chem. Phys.* **2006**, *124 (3)*, 034108.
12. Becke, A. D. Density-functional exchange-energy approximation with correct asymptotic behavior. *Phys. Rev. A Gen. Phys.* **1988**, *38 (6),* 3098-3100.
13. Lee, C.; Yang, W.; Parr, R. G. Development of the Colle-Salvetti correlation-energy formula into a functional of the electron density. *Phys. Rev. B Condens. Matter* 1**988**, 37 (2), 785-789.

14. Zhao Y.; Truhlar, D. G. The M06 suite of density functionals for main group thermochemistry, thermochemical kinetics, noncovalent interactions, excited states, and transition elements: two new functionals and systematic testing of four M06-class functionals and 12 other functionals. *Theor. Chem. Acc.* **2008**, *120 (1)*, 215–241.
15. Chai, J. D.; Head-Gordon, M. Long-range corrected hybrid density functionals with damped atom- atom dispersion corrections. *Phys. Chem. Chem. Phys.* **2008**, *10 (44)*, 6615-6620.
16. Kendall, R. A.; Dunning Jr., T. H.; Harrison, R. J. Electron affinities of the first-row atoms revisited. Systematic basis sets and wave functions,B *J. Chem. Phys.* **1992**, *96*, 6796-806.
17. Dunning Jr., T. H. Gaussian basis sets for use in correlated molecular calculations. I. The atoms boron through neon and hydrogen, *J. Chem. Phys.* **1989**, *90*, 1007-23.
18. Woon, D. E.; Dunning Jr., T. H. Gaussian-basis sets for use in correlated molecular calculations. 3. The atoms aluminum through argon, *J. Chem. Phys.* **1993,** *98*, 1358-71.
19. Chai, J.D.; Head-Gordon, M. Long-range corrected hybrid density functionals with damped atom-atom dispersion corrections, *Phys. Chem. Chem. Phys.* **2008**, *10*, 6615–6620.
20. Peterson, K. A.; Woon, D. E.; Dunning Jr., T. H. Benchmark calculations with correlated molecular wave functions. IV. The classical barrier height of the H+H2 → H2+H reaction, *J. Chem. Phys.* **1994,** *100*, 7410-15.
21. Purvis III, G. D.; Bartlett, R. J. A full coupled-cluster singles and doubles model – the inclusion of disconnected triples, *J. Chem. Phys.* **1982,** *76*, 1910-18.
22. Pople, J. A.; Head-Gordon, M. ; Raghavachari, K. Quadratic configuration interaction – a general technique for determining electron correlation energies, *J. Chem. Phys.* **1987**, *87*, 5968-75.
23. Johnson III, R. D. NIST Computational Chemistry Comparison and Benchmark Database. *NIST Standard Reference Database Number 101*, 2019.